ISPRS Open Journal of Photogrammetry and Remote Sensing 1 (2021) 100002

Contents lists available at ScienceDirect

ISPRS Open Journal of Photogrammetry and Remote Sensing

journal homepage: www.editorialmanager.com/OPHOTO

A decision-level fusion approach to tree species classification from multi-source remotely sensed data

Baoxin Hu [a,*], Qian Li [a], G. Brent Hall [b]

[a] Dept. of Earth and Space Science and Engineering, York University, 4700 Keele Street, Toronto, ON, M3J1P3, Canada
[b] Education and Research, Esri Canada, 900-12 Concorde Pl, Toronto, 4700, ON, M3C 3R8, Canada

ARTICLE INFO

Keywords:
Information fusion
Dempster Shafer Theory (DST)
Tree species classification
Normalized entropy
Multi-source remotely sensed data
Object-oriented

ABSTRACT

In this study, an object-oriented, decision-level fusion method is proposed for tree species classification based on spectral, textural, and structural features derived from multi-spectral and panchromatic imagery and Light Detection And Ranging (LiDAR) data. Murphy's average method based on the Dempster Shafer theory (DST) was used to calculate the combined mass function for decision making purposes. For individual feature groups, the mass functions were calculated using the support vector machine (SVM) classification method. The species examined included Norway maple, honey locust, Austrian pine, blue spruce, and white spruce. In addition to these species, a two- or three-species compound class was included in the decision process based on the normalized entropy in the presence of conflict that was itself determined according to whether individual groups of features were consistent. The developed method provided a mechanism to identify tree crowns, which could not be classified to one single species with a high confidence due to the conflict among feature groups. Data used in this study were obtained for the Keele Campus of York University, Toronto, Ontario. Among the 223 test crowns, 204 crowns were assigned to one single species, and the overall classification accuracy was 0.89. A decision could not be made for 19 crowns with confidence, and as a result, a two- or three-species compound class was assigned. The classification accuracy was higher than that obtained using SVM classification based on individual and combined spectral, structural, and textural features.

1. Introduction

Accurate identification of tree species is critically important for forest inventory and sustainable management of forest biomass. In urban environments, accurate tree species classification is needed for maintaining high biodiversity in urban forests that contributes, amongst other things, to improving urban ecology, reducing air, water and noise pollution, and helping to mitigate climate change (Iovan et al., 2008). Although tree species classification using remotely sensed data could be traced back to the beginning of remote sensing, it remains at this time an imprecise science. This is mainly due to the complexity of forest canopies in terms of their physical and biophysical properties, along with the on-going limitations of remotely sensed data (Hu et al., 2008). Trees of the same species may exhibit different properties between locations and sometimes within the same location. Moreover, trees of different species may show similar properties in remotely sensed data, contributing to the complexity of accurate species identification. This is likely true with some features individually, such as spectral signatures, which are commonly used in remote sensing classification. However, this problem may be minimized when several types of features are examined together.

Recent advances in remote sensing technologies have made a huge amount of data from different sensors, such as high spatial resolution imagery and high point density LiDAR (Light Detection and Ranging), readily available. These high spatial resolution data allow researchers to take advantage of the spatial and structural features of individual tree crowns in tree species classification in addition to the commonly used spectral signatures (Zhang and Hu, 2012; Alonzo et al., 2014; Li et al., 2015). Furthermore, individual tree crowns can be considered as the basic units with high spatial resolution data, which provide a flexible platform to integrate information from different data sources. In addition, it is relatively easier to register data at the individual crown level than at the individual pixel level. Furthermore, for individual tree crown (object)-based classification, resampling all data sources to the same spatial resolution may not be required.

The use of multi-source remotely sensed data also challenges researchers to develop effective methods to utilize fully all available

* Corresponding author.
E-mail addresses: baoxin@yorku.ca (B. Hu), qian2018@yorku.ca (Q. Li), bhall@esri.ca (G.B. Hall).

https://doi.org/10.1016/j.ophoto.2021.100002
Received 26 March 2021; Received in revised form 12 July 2021; Accepted 19 July 2021
Available online 22 July 2021

information of individual tree crowns in species classification. Data obtained from different sensors with the same properties can be redundant if they cover the same area. However, they can also be complementary if the sensors measure different physical properties of individual tree canopies. In addition, information provided by individual data sources is often imprecise and uncertain. Hence, the fusion of redundant and complementary data may provide a complete description of a given crown while reducing imprecision and uncertainty. Although studies have shown the potential to combine features from multi-source remotely sensed data in improving tree species classification (for example, Fassnacht et al., 2016), further investigation is required to achieve a full understanding of the discriminant powers of individual datasets and to seek an efficient and effective way to combine information from different sources.

The fusion of data from different sensors for classification usually occurs at either the feature or the decision level (Fassnacht et al., 2016). For feature-level fusion, features derived from individual sensors are consolidated into a single feature set. Machine-learning methods, such as support vector machine (SVM) (Cortes and Vapnick, 1995) and random forest (Ho, 1995), are commonly used to classify the species of interest based on the combined feature set. The SVM and random forest methods are generally shown to be more robust for classification with a large number of features in comparison with traditional parametric methods, such as maximum likelihood classification (Maxwell et al., 2018). However, the high dimensionality in the feature space that results from feature-level fusion is likely to be a concern for applications where the size of training samples is small (Maxwell et al., 2018). In addition, features derived from different data sources are usually treated equally by the SVM and random forest methods, even though some of the data sources may be more reliable than others. On the contrary, each data source is analyzed separately at the decision-level fusion, and the uncertainty and imprecision associated with each data source can be measured and considered in the fusion process. In this study, we focus on decision-level fusion.

Several methods have been developed for decision-level fusion in remote sensing classification. For example, Mora et al. (2011, 2012) employed Dempster Shafer theory (DST) (Dempster, 1968; Shafer, 1976) for species classification using satellite imagery, topographic information, and fire disturbance history records, and the mass function corresponding to each data source was determined by a Fuzzy Statistical Expectation Maximization (FSEM) method (Germain et al., 2002) or an empirical statistics analysis. Mora et al. (2011, 2012) also assumed a multivariate normal distribution, which might not always be true with features derived from remotely sensed data. Stavrakoudis et al. (2014) and, more recently, Aval et al. (2019) carried out a SVM classification to acquire the posterior-probability that a given target belonged to a certain tree species, and the final decision was made based on the weighted average of the probabilities from individual sources. With these methods (Stavrakoudis et al., 2014; Aval et al., 2019), the same species classes were used for all data sources and all targets (either individual pixels or crowns), and the posterior probabilities were calculated using the method proposed by Platt (1999) for binary classes and extended by Wu et al. (2004) for multiple classes. Bigdeli et al. (2014) used the SVM method for classification based on individual data sources, and a Naïve Bayes classifier was proposed to combine the classification results obtained based on individual data sources using the SVM method.

Although satisfactory results are reported in these studies, further research and in-depth analysis are warranted. One specific issue that needs to be addressed is classification uncertainty. For example, in the research noted above, a one-species class is ultimately assigned to a given sample based on a pre-determined criterion, such as a maximum probability or mass function, even though its value may not be significantly different between two different species, which makes the classification method not robust, especially in the presence of noise. Furthermore, based on different data sources, classification results may be different, due to conflict among data sources. Conflicting information presented by different data sources is not explicitly addressed in the existing methods. Based on DST, many methods have been developed to measure the conflicts among bodies of evidence and to deal with conflicting information (Zadeh, 1986; Yong et al., 2004). However, these methods are all statistics-based, and the generated results might not be intuitive in some cases. A detailed example is presented in the discussion section of this paper as an illustration. In the context of species classification or in the broader context of classifications using multi-source remotely sensed data, there is no generally accepted in-depth analysis to the best of our knowledge of the nature of conflicts or an effective method that should be used to measure and deal with conflicts.

To address the abovementioned issues related to classification uncertainty and conflicting information, this study exploits fully the discriminant power of two available data sources in individual tree species classification based on SVM classification and DST. Conflicts associated with different bodies of evidence are analyzed in detail and explicitly addressed. A framework is developed to classify a given crown into a two- or three-species compound. The developed method is validated using data obtained from high spatial resolution and multi-spectral imagery and LiDAR (Light Detection and Ranging) data over a study area in the city of Toronto, Ontario, Canada.

2. Study area and data pre-processing

The study area is located on the Keele campus of York University, Toronto, Canada (centered at 43.7735° N, 79.5019° W), as shown in Fig. 1. A number of trees grow along roads and in woodlots in the 457 acres of land. Campus Services and Business Operations (CSBO) at York University carried out tree inventory on the campus in June 2015. The location, species, diameter at breast height (DBH) and height were recorded for each tree. Although the tree inventory has not been updated recently, the acquired time frame matches that of the remotely sensed data used. In addition, the York University Map Library provided 8-centermeter resolution aerial image obtained in 2016 for study area (Fig. 1). This was used as a visual reference image to identify trees and double check the selected reference samples.

Five common species were selected for this study: Norway maple (*Acer platanoides*), honey locust (*Gleditsia triacanthos*), Austrian pine (*Casuarina equisetifolia*), blue spruce (*Picea pungens*), and white spruce (*Picea glauca*). A total of 751 trees were randomly selected. These trees were located along streets and near buildings and other high-pedestrian areas, thereby representing the typical distribution of trees in an urban area. The sampled trees included 188 Norway maples, 180 honey locusts, 159 Austrian pines, 115 blue spruces, and 109 white spruces. Of the 751 tree samples, 528 (around 70%) were used randomly for training and the remainder (223 trees) for testing. The characteristics of individual tree crowns commonly used by photo interpreters for the species of interest were compiled, and they could be potentially represented by spectral, textural, and structural features derived from the remotely sensed data. A summary is shown in Table 1.

Remotely sensed data available for this study included Worldview-2 (WV-2) imagery obtained on July 21, 2016, and airborne LiDAR data acquired in April 2015. The WV-2 imagery included one panchromatic band with a spatial resolution of 0.4 m by 0.4 m and eight multi-spectral bands with a spatial resolution of 1.6 m by 1.6 m. The WV-2 imagery was converted to surface reflectance by removing the atmospheric effect by using the Atmospheric & Topographic Correction (ATCOR) model in PCI Geomatics software (PCI Geomatics, Canada). The false color composite of the WV-2 imagery is shown in Fig. 2. The LiDAR data were collected using a Leica ALS 70 LiDAR instrument at a flying height of 1300 m with a Pulse Rate Frequency of 400 kHz, generating a point density of 10 points per square meter (Airborne Imaging Inc, Canada). The horizontal and vertical accuracies of the collected LiDAR data were 30 cm and 10 cm, respectively. A digital elevation model (DEM) and digital surface model (DSM) with the same spatial resolution as the WV-2 panchromatic band were generated from the LiDAR data cloud using Esri's ArcGIS

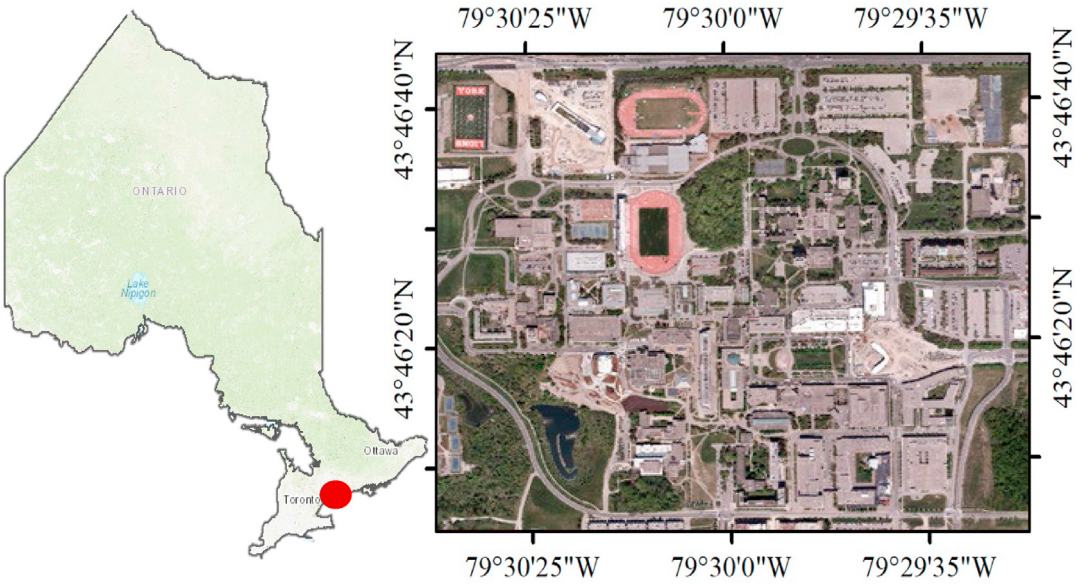

Fig. 1. The location indicated by the red dot (left) and an aerial photo (right) of the study area. (For interpretation of the references to colour in this figure legend, the reader is referred to the web version of this article.)

Table 1
Characteristics of tree crowns of the species of interest used in photo interpretation and potential remote sensing features.

Species	Leaf and its color	Crown texture	Crown size and shape
Norway maple	Simple leaf and dark green	Densely limbed, broad, rounded crown with sparse, dark holes	Growing to 20–30 m tall with a trunk up to 1.5 m in diameter, round or oval shaped
Honey locust	Compound leaf and bright green	Broad, flat-topped crown fuzzy/airy	Oval or round, spreading shaped with angular branches
Austrian pine	Simple needle-like parallel leaf and dark green	Coarse, patchy, prominent	Tall columnar shaped
Blue spruce	Stiff and sharp needle attached individually and evenly to branches, and blue-green in color	Sharp or dense	Pyramidal or conical shaped, typically grows to 12–18 m in height and 30–60 cm in trunk diameter
White spruce	Short, stiff, needles, and bluish green or green in color, with a whitish powdery, waxy layer	Very dense and symmetrical	In open grows conical, spire-like crown, with a rounded top; In dense stands, branches are self-pruning, coarser branching
Remote sensing features	Spectral from multi-spectral imagery	Statistical textural features from very high spatial resolution imagery	Canopy height and vertical profile features from LiDAR data

software. Corresponding to the DSM, the LiDAR in the intensity image was also generated. A canopy height model (CHM) was then derived as the difference between the DSM and DEM. The WV-2 imagery and LiDAR CHM were co-registered using the ortho-rectification method in ENVI software (Exelis Visual Information Solutions) via the LiDAR DSM and intensity image based on 400 manually selected tie points. These tie points were located at various elevations (on the ground or on buildings) and were evenly distributed across the study area. The resulting co-registration accuracy was 0.57 pixels. The LiDAR CHM is shown in Fig. 3.

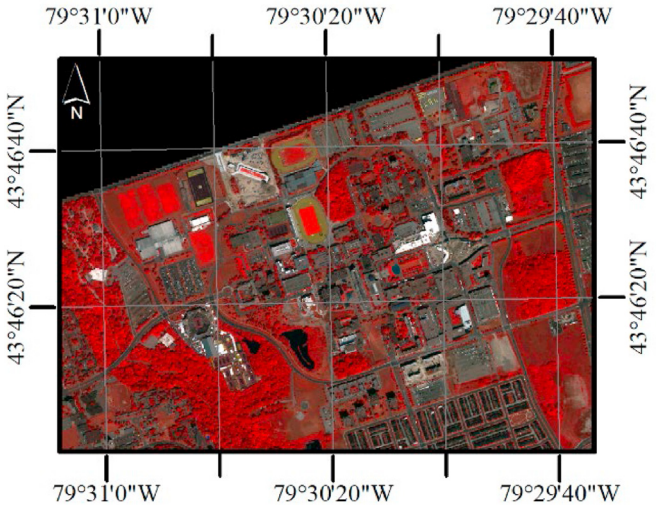

Fig. 2. The false color composite of the WV-2 imagery of the study area with the near-infrared band printed as red, red as green, and green as blue.(For interpretation of the references to colour in this figure legend, the reader is referred to the web version of this article.)

3. Method

Classification was performed on individual tree crowns, which were first delineated. Features were then derived from each crown for classification. Because the current study focused on the development of classification methods, the training and test crowns were manually delineated by visual interpretation based on aerial photos and information presented by both WV-2 imagery and LiDAR data. As shown in Fig. 4, spectral, textural, and structural features were extracted from WV-2 multi-spectral bands, WV-2 panchromatic band, and LiDAR data. SVM classification was then used to calculate the posterior probabilities of a given sample belonging to these five species based on individual feature groups. Decision fusion was finally carried out to classify a given tree crown to either one of the five species or a two-species or a three-species compound class. Details of the feature extraction, SVM classification, and decision fusion are described in the following subsections. Accuracy

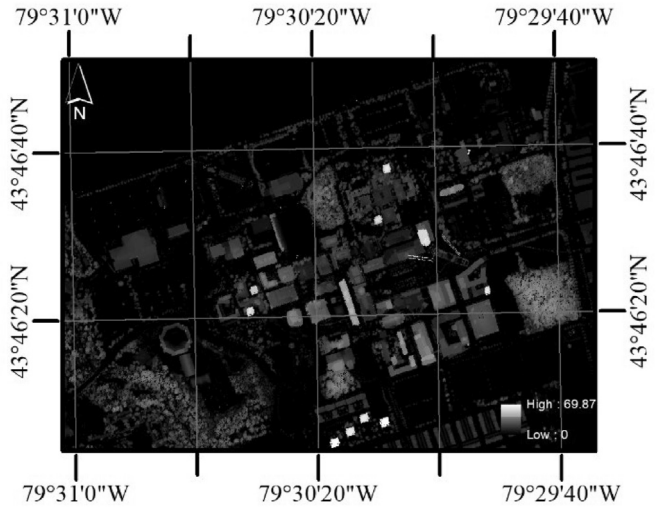

Fig. 3. The CHM derived from the airborne LiDAR data over the study area.

assessment is described as well.

3.1. Feature extraction

Based on the characteristics of individual tree crowns shown in Table 1, three categories of features were derived for species classification, including spectral features from the WV-2 multi-spectral bands (16), textural features from the WV-2 panchromatic band (11), and structural features from the LiDAR CHM and 3D data cloud (16). These features were calculated for each crown. As an example, Fig. 5 shows an individual tree crown exhibited from left to right in multi-spectral, panchromatic imagery of WV-2 and LiDAR CHM.

For the spectral features, the mean and standard deviations of the reflectance in the eight WV-2 multi-spectral bands were derived since trees with different species tend to have different spectral signatures.

As shown in Table 1, the tree crowns of the five species studied have different structures in leaf and branch distribution, which may be exhibited by high spatial resolution imagery as horizontal spatial patterns. In this study, the Gray Level Co-occurrence Matrix (GLCM) (Haralick et al., 1973) statistics were calculated based on the WV-2 panchromatic band (with a spatial resolution of 0.6 m by 0.6 m). For each tree crown, a GLCM was obtained with the displacement of 1 pixel, and all directions considered. In addition to the measures presented in Haralick et al. (1973), two cluster parameters, namely cluster shade and cluster prominence (Conners et al., 1984), were also considered to account for the perceptual concepts of uniformity and proximity. Eleven measures were selected and are summarized in Table 2. It is worth mentioning that a GLCM was calculated for individual crown segments. Due to the sizes of the crowns being different, the number of pairs of pixels that were considered to calculate the GLCM might be different. In this study, the displacement of 1 pixel was selected to ensure that there were sufficient numbers of pairs for the calculation even for small crowns. In addition, the displacement of more than 1 pixel was used to assess (a) if a value of other than 1 pixel for the displacement performed better in terms of the separation among species, and (b) if it was necessary to use measures from GLCMs calculated based on different displacements. The experimental results supported the use of the displacement of 1 pixel.

To characterize the vertical profiles and general structures of individual tree crowns, LiDAR CHM was first used to derive the general structural features, such as the mean and standard deviation in the height of a tree crown and the ratio of the maximum height to the projected area of the crown.

The fraction and distribution of tree elements, such as leaves and branches, within a tree crown or within-crown gaps tended to be different for different species (Li et al., 2013). There were four returns recorded for the LiDAR data used. Within tree canopies, the majorities of the returns were the first and the second. As a result, the proportions of the first two returns over the total returns within individual tree crowns subtracted from 1 were employed as two measures for with-crown gap fractions (1-proportions). The vertical profile of LiDAR points within a tree crown was used to reveal the distributions of the tree elements. A summary of the LiDAR features used is provided in Table 3.

The abovementioned features were selected from many candidates that have been reported in the literature to describe spectral, textural, and structural features from remotely sensed data based on prior knowledge. Analysis was also carried out to ensure that the features used were not highly correlated. Several feature selection methods are being applied in a separate study (Li, 2021) and the features used here were consistent with its result. These features were derived for individual crowns and their values were normalized between 0 and 1.

3.2. SVM classification

In this study, four SVM classifications were carried out. For the proposed method, an SVM classifier was first trained on each of the spectral, structural, and textural features. For comparison purposes, the fourth SVM was trained using the combined features used in the first three classifiers.

The SVM was implemented in MATLAB (version R2020a). A hard SVM was chosen over a soft SVM, since it was not trivial to seek the optimal value of the cost for a soft SVM and the value was not always the same for classifications using different features. The SVM was originally introduced as a binary classifier (Cortes and Vapnik, 1995), and to apply the SVM to multi-classes, the one vs. one strategy was used. For any pair of classes, the discriminant function was determined by Equation (1) as

$$y = \sum_{i=1}^{m} \alpha_i y_i K\left(\vec{x}_i^T \vec{x}\right) + b,\ K\left(\vec{x}_i^T \vec{x}\right) = -\gamma e^{-\vec{x}-\vec{x}_i^2}, \tag{1}$$

where m is the number of support vectors; $\vec{x}_i$ and y_i are the feature vector and label of support vector i; K is the kernel function; and α and b are the parameters determined through the training process. The Gaussian radial basis function (RBF) was used as the kernel and its format is provided as well. For the RBF kernel, there is one parameter, γ, which defines the extent of the influence of a single training example can reach. In this study, it was set as the inverse of the number of training samples.

A large absolute value in y (greater than 1) represents a confident prediction, and a value of 0 for y means that the unknown vector is on the hyperplane that separated the two classes, leading to maximum prediction uncertainty. The posterior probabilities that a given sample belonged to these two classes were obtained by implementing modified Platt Scaling (Platt, 1999) used by Lin et al. (2007). As noted earlier, five species classes were used in this study, and as a result ten binary SVM classifiers were built. The posterior probabilities of a given sample belonging to these five species were calculated (Wu et al., 2004) and employed as the mass functions for the decision-level fusion based on DST.

3.3. Decision fusion

For the decision-level fusion, Murphy's average approach (Murphy, 2000) was used instead of the more commonly used Dempster's rule of combination (Shafer, 1976). The justification for its use is described later in this subsection. Murphy's average approach is built on Dempster's rule of combination, which is shown in Equation (2),

$$m(A) = \frac{\sum_{B_1 \cap \ldots \cap B_n = A} m_1(B_1) \ldots m_n(B_n)}{1 - \mathrm{K}}, \quad K = \sum_{B_1 \cap \ldots \cap B_n = \varnothing} \prod_{i=1}^{n} m_i(B_i), \tag{2}$$

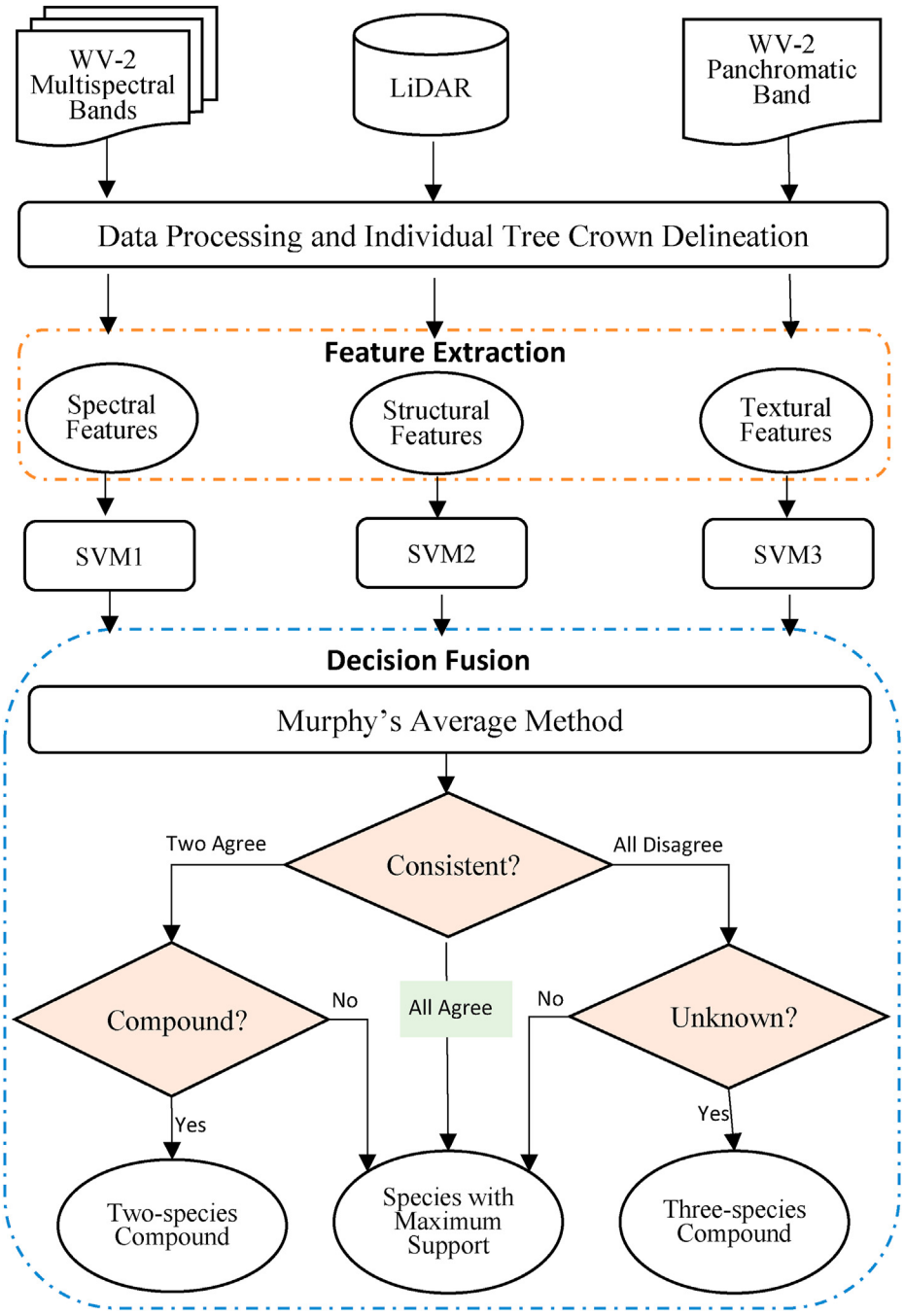

Fig. 4. The workflow of the developed method.

where $m(A)$ is the mass function of a proposition A after considering n pieces of evidence; $m_i(B_i)$ is the mass function in the proposition B_i supported by the ith piece of evidence; and K is known as the total conflict factor.

Based on Dempster's rule of combination, the mass function for proposition A can be interpreted as the accumulated evidence supporting this proposition normalized by that supporting all non-null propositions. As the data become more contradictory (pieces of evidence strongly support contradictory propositions), K approaches 1, and a combination of the data is less logical. As a result, Dempster's rule of combination is not effective in situations where evidence or information sources are conflicting and may generate counterintuitive results (Zadeh, 1986). With Murphy's average approach, the mass functions corresponding to all evidence are first averaged, and Dempster's rule of combination is then applied to the average to get the combined mass function. To demonstrate the difference between these two combination methods and to understand better the rationale behind the proposed method, three cases are shown in Tables 4–6 as examples. They corresponded to three scenarios: (1) there were no conflicts among the three types of features (that is, the same result was obtained from the SVM classification based on the three features individually); (2) two types of features were highly conflicting; and (3) three different species classes were supported by the three types of features.

For the first case (Table 4), the species with the maximum support from the spectral, structural, and textural features was the same. Thus, there was no conflict among the feature groups. In this case, both combination rules provided similar results. For the other two cases with conflicts among feature groups, the results from Murphy's average

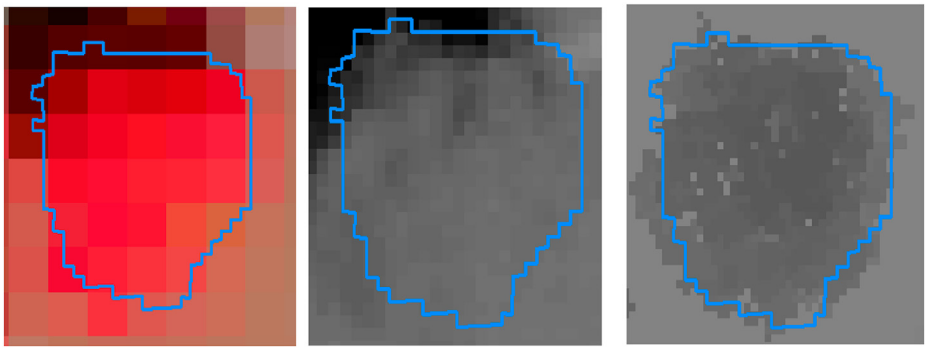

Fig. 5. An individual tree crown on the false color image of the WV-2 multi-spectral bands (left), WV-2 panchromatic band (middle), and LDAR-derived CHM (right). (For interpretation of the references to colour in this figure legend, the reader is referred to the web version of this article.)

Table 2
Textural features utilized in this study.

Features	Formula
Entropy	$-\sum_i\sum_j[p(i,j)\log p(i,j)] = H_{xy}$
Information measures of correlation 1	$\frac{H_{xy}-H_{xy1}}{\mathrm{Max}\{H_x,H_y\}}$ $H_{xy1} = -\sum_i\sum_j[p(i,j)\log(p_x(i)p_y(j))]$ $H_x = -\sum_i[p_x(i)\log p_x(i)]$ $H_y = -\sum_j[p_y(j)\log p_y(j)]$
Information measures of correlation 2	$(1-\exp[-2(H_{xy2}-H_{xy})])^{\frac{1}{2}}$ $H_{xy2} = \sum_i\sum_j[p_x(i)p_y(j)\log(p_x(i)p_y(j))]$
Difference entropy	$-\sum_k[p_{x-y}(k)\log p_{x-y}(k)]$, $p_{x-y}(k) = \sum_i\sum_j p(i,j)$ $\lvert i-j\rvert = k$
Correlation	$\frac{\sum_i\sum_j[(ij)*p(i,j)]-\mu_x\mu_y}{\sigma_x\sigma_y}$
Sum variance	$\sum_{i=2}^{2N}(i-f)^2p_{x+y}(i)$; $-\sum_{i=2}^{2N}p_{x+y}(i)\log\{p_{x+y}(i)\} = f$
Cluster shade	$\sum_i\sum_j[(i+j-\mu_x-\mu_y)^3*p(i,j)]$
Cluster prominence	$\sum_i\sum_j[(i+j-\mu_x-\mu_y)^4*p(i,j)]$
Maximum probability	$MAX\{p(i,j)\}$
Inverse difference	$\sum_i\sum_j\frac{p(i,j)}{1+\lvert i-j\rvert}$
Inverse difference momentum	$\sum_i\sum_j\frac{p(i,j)}{1+(i-j)^2}$

$p(i,j)$ is the (i,j) entry in a normalized GLCM; $p_x(i)$ is the ith entry of the marginal probability matrix obtained by summing the rows of the matrix p; $p_y(j)$ is the jth entry of the marginal probability matrix obtained by summing the columns of the matrix p; and μ_x,μ_y,σ_x, and σ_y are the mean and standard deviations of the matrix of p_x and p_y.

Table 3
Structural features derived from LiDAR point cloud and CHM.

Type	Description	Number of metrics
General structure	Mean and standard deviation of heights within a crown and the ratio of the maximum height to the projected area	3
Gap fraction	Fractions of first and second returns within individual tree crowns	2
Vertical profile	Proportion of LiDAR points per horizontal layer to total number of points within individual tree crown, considering 10 equal thickness layers along the vertical profile. The first five were used.	5

method were more reasonable. Specifically, as shown in the second scenario (Table 5), according to the SVM classification based on spectral and structural features, the tree crown of interest belonged to honey locusts and Austrian pines, respectively, both with a very high degree of belief (0.964 and 0.946, respectively). A decision could hardly be made based on these two pieces of conflicting evidence. For the third piece of evidence (textural feature, Table 5), the mass function from the SVM classification was also close between honey locusts and Austrian pines (0.449 and 0.539, respectively). From these results, it would be reasonable to conclude that this tree crown might belong to Austrian pines, but the uncertainty in this decision would be high. The result based on Murphy's average method was consistent with our intuition, while based on Dempster's rule, there was strong evidence that this tree crown

Table 4
The decision fusion results using Dempster's combination rule and Murphy's average method: Case A. The Norway maple, honey locust, Austrian pine, blue spruce, and white spruce are denoted as MN, LH, PA, SB, and SW, respectively.

Evidence (features)	Mass function				
	MN	LH	PA	SB	SW
Spectral	0.787	0.116	0.010	0.015	0.072
Structural	0.967	0.024	0.009	0.000	0.000
Textural	0.946	0.005	0.021	0.011	0.017
Dempster's rule	1.000	0.000	0.000	0.000	0.000
Murphy's method	1.000	0.000	0.000	0.000	0.000

Table 5
The decision fusion results using Dempster's combination rule and Murphy's average method: Case B. The Norway maple, honey locust, Austrian pine, blue spruce, and white spruce are denoted as MN, LH, PA, SB, and SW, respectively.

Evidence (features)	Mass function				
	MN	LH	PA	SB	SW
Spectral	0.021	0.964	0.001	0.006	0.008
Structural	0.000	0.005	0.946	0.024	0.024
Textural	0.004	0.449	0.539	0.001	0.007
Dempster's rule	0.000	0.803	0.196	0.000	0.001
Murphy's method	0.000	0.465	0.535	0.000	0.000

Table 6
The decision fusion results using Dempster's combination rule and Murphy's average method: Case C. The Norway maple, honey locust, Austrian pine, blue spruce, and white spruce are denoted as MN, LH, PA, SB, and SW, respectively.

Evidence (features)	Mass function				
	MN	LH	PA	SB	SW
Spectral	0.006	0.234	0.055	0.151	0.554
Structural	0.000	0.816	0.002	0.094	0.087
Textural	0.000	0.001	0.000	0.609	0.390
Dempster's rule	0.000	0.006	0.000	0.310	0.684
Murphy's method	0.000	0.403	0.000	0.215	0.381

belonged to honey locust (with a belief of 0.803).

To understand further the nature of the classification results based on these three groups of features, the SVM binary classification between honey locusts and Austrian pines was checked. As shown in Table 7, for the binary classification between honey locusts (positive class) and Austrian pines (negative class), the discriminant function in Equation (1) had the values of 3.942, −3.925, and −0.019 based on spectral, structural, and textural features, respectively. The SVM classifier based on the spectral and structural features categorized this crown as honey locusts and Austrian pines, respectively, with high confidence (with the y value much higher than 1 or -1). However, the y value was close to 0 for the SVM classifier based on textural features, and thus the classification uncertainty was very high. For this case, a reasonable decision would be to assign this crown to a compound class of honey locust and Austrian pine.

For the case shown in Table 6, the spectral, structural, and textural features supported different species classes (white spruce, honey locust, and blue spruce, respectively). According to Dempster's combination rule, there was relatively strong combined evidence to support the proposition that this crown belonged to a white spruce (0.608). However, based on Murphy's average method, there was a similar level of weak support for the proposition that this crown belonged to either honey locust (0.403) or white spruce (0.381), which was supported by the results from the three binary SVM classifications involved for the three possible species classes (Table 8).

Between the honey locust and the blue spruce, this crown belonged to both species with a high confidence (the absolute discriminant function greater than 1) based on structural and textural features, respectively. Between the honey locust and the white spruce, the absolute discriminant function had a value greater than 1 based on the structural and textural features, meaning there was strong evidence to support a decision for honey locust and white spruce. Between the blue spruce and the white spruce, the absolute discriminant function had a value smaller than 1, which could be interpreted as two votes of weak support for the white spruce and one vote of stronger support for the blue spruce. Hence, based on the spectral, structural, and textural features, a decision on any single species among the honey locust, blue spruce, or white spruce could not be made with high confidence. As a result, a three-species compound class would be a suitable choice.

Based on the results presented in the examples shown in Tables 4–6, Murphy's method was used for this study. These examples also indicated that compound classes might need to be introduced due to relative species uncertainty. In the existing classification methods based on DST, the decision is often made based on the maximum pignistic probability (Smets, 2000), and uncertainty in the decision is characterized by the range between belief and plausibility. For the case in this study with only single propositions (singletons), the decision based on pignistic probabilities is the same as that based on mass functions, and an uncertain range is not defined. Hence, we used the following logic in the decision making process considering the abovementioned three cases.

For each feature group, assign the species to the one with the maximum mass function. In the first case (as in Table 4), the results were consistent among the three feature groups. The species with the maximum combined mass function calculated using Murphy's average method was assigned to this crown, and the normalized entropy (normalized over the maximum entropy) was calculated over the mass functions of the five species. The normalized entropy served as an uncertainty measure (Pittman et al., 2021). For the second case (as in Table 5), the classification result for one feature group was different from the other two. This crown could be either honey locus or Austrian pine. The normalized entropy was then calculated based on the mass functions of the two species. If the entropy was high (above 0.95), the compound proposition consisting of these two species was assigned to the crown of interest. Otherwise, the species with the highest combined mass function was assigned as in the first case. For the third case (as in Table 6), each feature group supported one different species based on the maximum mass function. This crown could be either white spruce, honey locust, or blue spruce, and as a result, the normalized entropy was calculated based on the mass functions associated with these three species. If the entropy was high (above 0.95), the compound proposition consisting of these three classes was assigned, and otherwise, the species with the highest combined mass function was chosen as in the first two cases.

Table 7
The discriminant function (y-value) from the binary SVM classifier between the honey locust (positive class) and Austrian pine (negative class) based on spectral, structural, and textural features for Case B (Table 5).

Evidence (features)	Spectral	Structural	Textural
y_value	3.942	−3.925	−0.019

Table 8
The discriminant function (y-value) from the binary SVM classifier based on spectral, structural, and textural features for Case C (Table 6). In each binary SVM listed, the first species class is the positive class and the second the negative class.

Evidence (features)	y_value (binary SVM)		
	LH vs. SB	LH vs. SW	SB vs. SW
Spectral	0.619	−0.579	−0.929
Structural	1.471	1.192	0.398
Textural	−4.128	−4.710	0.312

The use of entropy as an uncertainty measure for classification problems is not new (e.g., Pittman et al., 2021). However, it has been commonly calculated over all species of interest, and hence did not measure the uncertainty between two or three species where uncertainty occurred. As a demonstration, from the analysis for the case listed in Table 5, a decision could not be made between the honey locust and Austrian pine. If the entropy was calculated based on the mass functions of the five species, the normalized value was 0.47 according to Murphy's average method, which was not high. If the entropy was calculated based on only the honey locust and the Austrian pine, the normalized value was 0.99, which was very high. Similarly, for the case shown in Table 6, the normalized entropy values for the five and three species were 0.66 and 0.97, respectively. Based on the normalized entropy approach proposed in this study, the tree crown in Table 5 was assigned as a compound of honey locust and Austrian pine and the one in Table 6 as a compound of honey locust, blue spruce, and white spruce.

It is worth mentioning that the threshold of 0.95 in the normalized entropy was chosen by considering the discriminant functions (y – values) of the SVM classification for various cases. For the third case, there were many scenarios of conflict and uncertainty. It was difficult to establish the criteria to determine whether a compound class was appropriate based on the discriminant functions. The situation gets worse for classifications using a large number of feature groups. As a trade-off between algorithm complexity and physical significance, the normalized entropy was used, and its calculation was adapted to these three cases.

3.4. Accuracy assessment

To evaluate the proposed method, the test samples were classified. The numbers of test crowns that were classified into one species and two-species or three-species compound were tallied. For the crowns classified into one species, the confusion matrix was calculated. The user's accuracy, producer's accuracy, overall accuracy, and kappa coefficient were calculated. For comparison with the fusion method at the feature level, one single species was also assigned to each of the tests, based on the maximum mass function based on the maximum mass function and the confusion matrix and corresponding accuracies were calculated. The overall accuracy was also calculated for the SVM classification using the spectral, structural, and textual features individually and combined.

4. Results and analysis

The spectral features (mean and standard deviation) for a sample tree crown are shown in Fig. 6. There were some differences in the mean reflectance among the five species, but as expected, the difference might not be sufficient to be used alone to discriminate between these species. It is also noted that the difference in the standard deviation in the reflectance for the whole crown was relatively larger compared with that for the mean reflectance. This indicates that the difference in the vertical and horizontal structures of tree crowns might be revealed in the standard deviation. Most of the textural measures examined in this study are commonly used, but cluster prominence and cluster shade are rarely employed. These two features, shown in Fig. 7, were able to show the characteristics of gaps and shadows within crowns, which tended to be different among the five species. Although the horizontal and vertical structures of tree crowns were evident in the spectral and textural features, they were characterized in detail with the features derived from LiDAR data. Fig. 8 shows the gap fractions derived from the LiDAR data for a tree crown.

The classification results based on the 223 test tree crowns are shown in Tables 9–12. With these results, conflict was determined based on whether the decisions made were consistent across individual groups of features. For three groups of features, one, two, or three species could be supported based on the maximum posterior probabilities generated from the SVM classifiers. As shown in Table 9, among the 223 test samples, there were 105 crowns where all feature groups supported the same species (labeled as "all agree"); 101 crowns (96% of them) were assigned correctly to one single species, and only four crowns were misclassified. Even for the misclassified crowns, the species being assigned had strong combined support according to these features. For these crowns, additional information was required. For example, temporal features could be used to separate deciduous and coniferous species. Most of the Norway maple crowns fell into this category. For the case where two types of features supported one species and the third was not (labeled as "Two agree"), there were 98 tree crowns. Of these, 82 crowns were assigned to one single species with 85% (70 crowns) correct, and 16 crowns were determined as uncertain between two species and classified as a two-species compound class.

For the case where each type of feature supported different species based on the SVM classification (labeled as "all disagree"), there were 21 tree crowns. Of these, 17 were assigned to one single species with 65% of them (11 crowns) correct, and three tree crowns were identified as a compound class. An expected decrease in the overall accuracy in the presence of conflicts is apparent. Honey locust, blue spruce, and white spruce appeared more in the compound classes. The uncertainty between the blue spruce and white spruce is logical because they belong to the same genus.

Table 10 shows the confusion matrix of the classification results for the 204 total test crowns assigned to one single species. The overall accuracy was 0.89. The user's accuracy was high for all species, but the

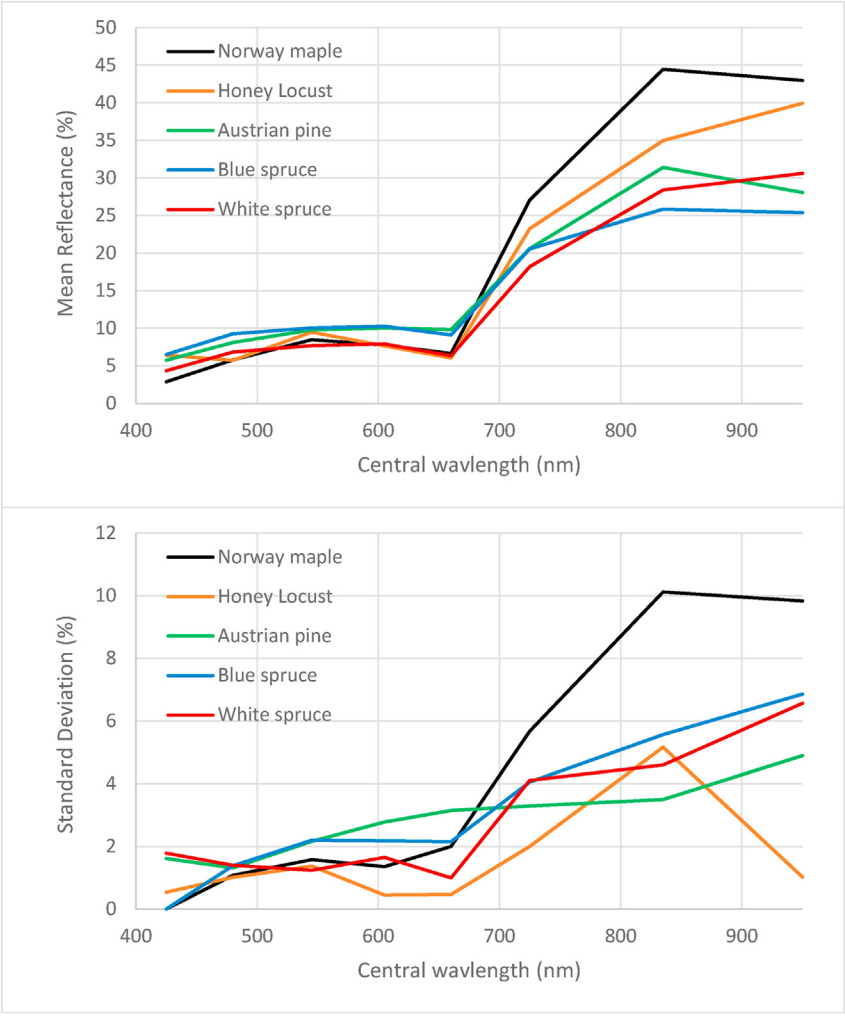

Fig. 6. The mean (top panel) and standard deviation (bottom panel) of the reflectance in the eight WV-2 multi-spectral bands for individual tree crowns of species of interest.

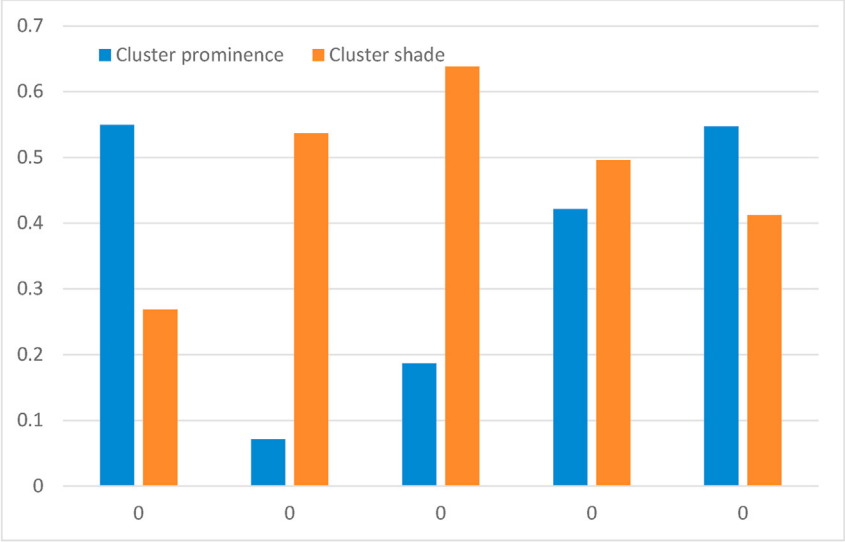

Fig. 7. The cluster prominence and cluster shade of an example tree crown for each species (the same crowns as those in Fig. 6) based on the WV-2 panchromatic band.

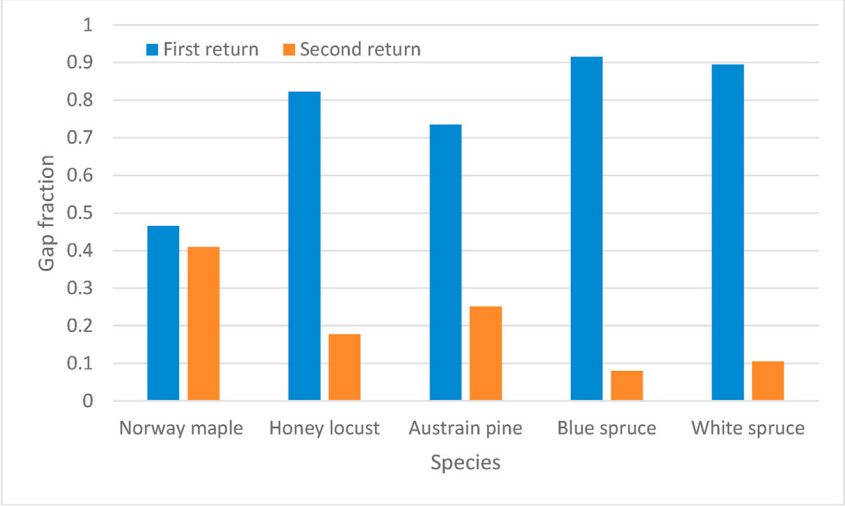

Fig. 8. The cluster prominence and cluster shade of an example tree crown for each species (the same crowns as those in Fig. 6) based on the WV-2 panchromatic band.

producer's accuracy for white spruce was low (0.55). Most of the misclassification occurred between blue spruce and white spruce.

In comparison, the confusion matrix for all test tree crowns, without excluding uncertain tree crowns based on the entropy measure, is shown in Table 11. The decrease in the overall accuracy when including all test crowns indicated that most uncertain tree crowns (compound) were very likely misclassified if the species with the maximum combined mass function was assigned. As analyzed in the previous section, for these tree crowns, the difference in the combined mass function between two or three species was small, and assignment to a species led to high uncertainty.

Table 9
The numbers of crowns that fell into each category and the classification status.

Categories	Number of crowns	Classified as single species		Classified as a compound class	
		Total crowns	Correctly classified	Total crowns	Correctly classified[a]
All agree	105	105	101	0	–
Two agree	98	82	70	16	12
All disagree	20	17	11	3	3
Total	223	204	182	19	15

[a] Meaning the species as the ground truth was included in the compound class.

The overall accuracies are shown in Table 12 to compare the classification results under different schemes. To produce Table 12, all test tree crowns were assigned to the species with the maximum posterior probability (for the SVM classifiers) and combined mass function (for decision-level fusion). As expected, the classification accuracies were higher by combining features together either at the feature level or at the decision level. Among the feature groups used, the classification accuracy was the highest for the structural features. The accuracy based on Murphy's average method at the decision level was slightly higher than that from feature-level fusion.

5. Discussion

The overall classification results obtained in this study (Table 12) are

Table 10
The confusion matrix for the crowns assigned to a single species. The Norway maple, honey locust, Austrian pine, blue spruce, and white spruce are denoted as MN, LH, PA, SB, and SW, respectively.

		Ground truth					Total	User's accuracy
		MN	LH	PA	SB	SW		
Classification	MN	54	2	0	0	0	56	0.96
	LH	1	47	2	3	2	55	0.85
	PA	0	0	44	1	2	47	0.94
	SB	0	0	0	25	6	31	0.81
	SW	0	1	0	2	12	15	0.80
	Total	55	50	46	31	22	Overall accuracy: 0.89	
	Producer's accuracy	0.98	0.94	0.96	0.81	0.55	Kappa coefficient: 0.86	

Table 11
The confusion matrix for all test tree crowns. The Norway maple, honey locust, Austrian pine, blue spruce, and white spruce are denoted as MN, LH, PA, SB, and SW, respectively.

		Ground truth					Total	User's accuracy
		MN	LH	PA	SB	SW		
Classification	MN	55	3	0	0	0	58	0.95
	LH	1	47	4	4	3	59	0.80
	PA	0	2	44	1	2	49	0.90
	SB	0	0	0	27	11	38	0.71
	SW	0	2	0	3	14	19	0.74
	Total	56	54	48	35	30	Overall accuracy: 0.84	
	Producer's accuracy	0.98	0.87	0.92	0.77	0.47	Kappa coefficient: 0.79	

Table 12
The overall accuracies (OA) using SVM classifiers based on spectral, structural, and textural features individually and combined and using Murphy's average method for the decision-level fusion.

Method	SVM classification				Decision-level fusion[a]	
	Spectral	Structural	Textural	Combined	Method 1	Proposed method
OA	0.69	0.77	0.71	0.81	0.85	0.89

[a] In the calculation of the OA for the proposed method, only the tree crowns assigned to a single species were considered. For method 1, uncertainty was not considered, and every tree crown was assigned to a single species.

consistent with the expectation and with the literature that multi-source remotely sensed data have advantages over individual data sources and that fusion at the decision level is promising compared that at the feature level in discriminating between tree species (Fassnacht et al., 2016). The uniqueness of this study in comparison with the existing methods reported in the literature is that instead of ultimately assigning one single species to an unknown tree crown, the normalized entropy approach was proposed to measure uncertainty and to assign potentially a compound class to the tree crown. Furthermore, the normalized entropy was calculated differently for different tree crowns based on whether the bodies of evidence generated conflicting classification results. As shown for the cases in Tables 5 and 6 and the corresponding analysis, the normalized entropy approach was effective and adaptive in characterizing classification uncertainty and in assigning a compound class.

It can be argued that based on DST, the compound propositions could be considered. There were two reasons that we did not consider them. Firstly, it was not conceptually and computationally easy to determine the mass functions for all possible compound propositions. Secondly, it was not necessary. For some tree crowns, such as the 105 test crowns (Table 9) without conflicts among the feature groups, there was no need for the compound classes. In this study, we attempted to include compound classes directly and to obtain their mass functions using SVM classifications as well. The preliminary results did not show much improvement compared with the proposed method, and further investigations are being pursued.

Hence, we propose the use of Murphy's average method instead of the commonly used Dempster's combination rule to generate more intuitive results in the presence of conflicts. In the calculation of the average mass function using Murphy's average method, the mass functions from individual groups of features were treated equally. In the literature, the weighted average has been used based on the confidence level for each piece of evidence (Stavrakoudis et al., 2014; Aval et al., 2019). The weight for each piece of evidence is commonly taken as the overall classification accuracy obtained based on individual groups of features.

For this study, as shown in Table 12, the accuracies obtained for the spectral, structural, and textural features were similar. Furthermore, the accuracies were calculated over all test samples and might not be appropriate for individual test samples. The confidence level could be measured for individual cases based on how the consistency of one piece of evidence compares with others, which is often calculated based on Jousselme's distance (Jousselme et al., 2001) defined in Equation (3),

$$d\left(\vec{m}_i, \vec{m}_j\right) = \sqrt{\frac{1}{2}\left(\vec{m}_i - \vec{m}_j\right)^T D\left(\vec{m}_i - \vec{m}_j\right)}, \tag{3}$$

where D is a k by k matrix; k is the number of focal elements, and it is an identity matrix for the set containing singletons. The conflict measure of evidence i can be further calculated as the average distance between this evidence and any other evidence.

Based on Jousselme's distance, Yong et al. (2004) and Liu et al. (2011) calculated the credibility degree and the relative weighting factor to weigh each piece of evidence in the calculation of the combined mass function. For the case shown in Table 5, spectral features conflicted with the structural and textural features that were indicated by the mass functions and confirmed by the conflict measure in Table 13. Among the three feature groups, textural features were more consistent with the

spectral and structural features. Consequently, the textural features were more credible and should be given more weight (Table 13). If Murphy's weighted method was used, the combined mass functions for the honey locust and Austrian pine were 0.383 and 0.617, respectively, and 0 for the other species. The same method generated more support for the Austrian pine than the "non-weight" one (Table 5).

As analyzed, the discriminant function between the honey locust and the Austrian pine based on the textural features was very close to 0 (−0.0193, slightly favored the Austrian pine, Table 7). The textural features might be credible based on their consistency with other features, but they might not be reliable based on the discriminant function. This example illustrates that caution should be exercised when using these statistics-based measures. Given these results, we recommend using the "non-weighted" average in the Murphy's method and evaluating the conflict among bodies of evidence based on the SVM classification result.

In this study, individual tree crowns were delineated manually to minimize the impacts of uncertainty in individual crown delineation on the classification results. Even though methods have been developed to delineate tree crowns automatically, the accuracy remains low. In future work, we will develop methods to integrate individual tree delineation and classification together in the workflow. Even though we are satisfied with the manually delineated crowns based on visual inspection, it is likely that the delineated crown boundaries might not exactly align with the real ones. However, since the spectral, structural, and textural features were mostly statistically based and calculated over a number of pixels within crowns, the minor shift between the delineated and true crown boundaries was not expected to affect the classification significantly. This will be further investigated in future work.

6. Conclusion

In this study, an object-oriented decision-level fusion method was used for tree species classification based on spectral, textural, and structural features derived from multi-spectral and panchromatic imagery and LiDAR data. Individual tree crowns served as the basic units, and remote sensing features extracted for each tree crown were used for SVM classification. Murphy's average method based on DST was used to calculate the combined mass function for decision making purposes.

The species of interest included the Norway maple, honey locust, Austrian pine, blue spruce, and white spruce. In addition to these species, a two-species or a three-species compound class could be assigned to a tree crown based on the normalized entropy in the presence of conflict. Among the 223 test samples, 204 were assigned to one single species, with an overall accuracy of 0.89. Furthermore, among the remaining 19 tree crowns where a compound class was assigned, the ground truth species was among the compound class for most cases. These results demonstrate the effectiveness of the proposed method.

Decision-level fusion was also shown to have a higher classification accuracy relative to feature-level fusion method and with the classification based on the spectral, textural, and structural features individually. Furthermore, with decision-level fusion, the conflict and uncertainty generated from individual bodies of evidence could be explicitly addressed.

With individual tree crowns as the basic units, the spatial and structural features were extracted and used in addition to the more commonly used spectral features in species classification. The addition of these features proved to be beneficial. However, the misclassification among the species indicated that additional information, such as temporal features, may be needed to minimize misclassification between deciduous species and coniferous species. There was also confusion evident in this study between the blue and white spruce. Very high spatial resolution imagery obtained by Unmanned Aerial Vehicles (UAVs) and very high-density LiDAR data can potentially be used to derive detailed spatial and structural features to improve the accuracy of correctly classifying different species from the same genus.

An in-depth analysis was carried out in this study to examine the impact of conflict and uncertainty among feature groups on decision making based on DST. It was shown that Murphy's average method can generate intuitive results in the presence of conflicts compared with the more commonly used Dempster's combination rule. Based on the in-depth analysis, conflict among bodies of evidence was determined according to the classification results based on individual groups of features, and the corresponding normalized entropy was calculated to decide whether one single species or a compound class was assigned to a given tree crown. The decision made based on this approach is consistent with the discriminant functions of the SVM classifications and the proposed method could be generalized to cases with more evidence. In future research, we plan to extend this method to include more classes of species integrated with the individual tree crown delineation method to map species automatically and over a larger area than that examined here.

Table 13
The conflict, credibility, and weight calculated for the case shown in Table 5.

Evidence	Conflict	Credibility	Weight
Spectral	0.739	0.238	0.271
Structural	0.689	0.284	0.321
Textural	0.477	0.478	0.407

Declaration of competing interest

The authors declare that they have no known competing financial interests or personal relationships that could have appeared to influence the work reported in this paper.

Acknowledgement

The authors would like to thank York University library and CSBO for the LiDAR and tree inventory data, respectively. We would like to acknowledge the financial support provided by the Natural Sciences and Engineering Research Council (NSERC) of Canada, Esri Canada, and Ontario Ministry of Agriculture, Food and Rural Affairs (OMAFRA). We would also like to thank Dr. Hui Li of York University and the Key Laboratory of Digital Earth Science, Aerospace Information Research Institute, Chinese Academy of Sciences for her help in the co-registration of the WV-2 imagery and LiDAR data.

References

Alonzo, M., Bookhagen, B., Roberts, D.A., 2014. Urban tree species mapping using hyperspectral and lidar data fusion. Rem. Sens. Environ. 148, 70–83. https://doi.org/10.1016/j.rse.2014.03.018.

Aval, J., Fabre, S., Zenou, E., Sheeren, D., Fauvel, M., Briottet, X., 2019. Object-based fusion for urban tree species classification from hyperspectral, panchromatic and nDSM data. Int. J. Rem. Sens. 40 (14), 5339–5365. https://doi.org/10.1080/01431161.2019.1579937.

Bigdeli, B., Samadzadegan, F., Reinartz, P., 2014. A decision fusion method based on multiple support vector machine system for fusion of hyperspectral and LIDAR data. Int. J. Image Data Fusion 5 (3), 196–209. https://doi.org/10.1080/19479832.2014.919964.

Conners, R.W., Trivedi, M.M., Harlow, C.A., 1984. Segmentation of a high-resolution urban scene using texture operators (Sunnyvale, California). Comput. Vis. Graph Image Process 25 (3), 273–310. https://doi.org/10.1016/0734-189X(84)90197-X.

Cortes, C., Vapnik, V., 1995. Support-vector networks. Mach. Learn. 20 (3), 273–297. https://doi.org/10.1007/BF00994018.

Dempster, A.P., 1968. Upper and lower probabilities generated by a random closed interval. Ann. Math. Stat. 39 (3), 957–966. https://doi.org/10.1214/aoms/1177698950.

Fassnacht, F.E., Latifi, H., Stereńczak, K., Modzelewska, A., Lefsky, M., Waser, L.T., Straub, C., Ghosh, A., 2016. Review of studies on tree species classification from remotely sensed data. In: Remote Sensing of Environment, vol. 186. Elsevier, pp. 64–87. https://doi.org/10.1016/j.rse.2016.08.013.

Germain, M., Voorons, M., Boucher, J.M., Benie, G.B., 2002. Fuzzy statistical classification method for multiband image fusion. In: Proceedings of the Fifth International Conference on Information Fusion. FUSION 2002. (IEEE Cat. No. 02EX5997), vol. 1, pp. 178–184. https://doi.org/10.1109/ICIF.2002.1021148.

Haralick, R.M., Shanmugam, K., Dinstein, I.H., 1973. Textural features for image classification. IEEE Trans. Syst. Man Cybern. 6, 610–621. https://doi.org/10.1109/TSMC.1973.4309314.

Ho, T.K., 1995. Random decision forests. In: Proceedings of 3rd International Conference on Document Analysis and Recognition, vol. 1, pp. 278–282. https://doi.org/10.1109/ICDAR.1995.598994.

Hu, B., Miller, J.R., Zarco-Tejada, P., Freemantle, J., Zwick, H., 2008. Boreal forest mapping at the BOREAS study area using seasonal optical indices sensitive to plant pigment content. Can. J. Rem. Sens. 34 (Suppl. 1), S158–S171. https://doi.org/10.5589/m07-066.

Iovan, C., Boldo, D., Cord, M., 2008. Detection, characterization, and modeling vegetation in urban areas from high-resolution aerial imagery. IEEE J. Select. Top. Appl. Earth Obs. Rem. Sens. 1 (3), 206–213. https://doi.org/10.1109/JSTARS.2008.2007514.

Jousselme, A.-L., Grenier, D., Bossé, É., 2001. A new distance between two bodies of evidence. Inf. Fusion 2 (2), 91–101. https://doi.org/10.1016/S1566-2535(01)00026-4.

Li, D., Ke, Y., Gong, H., Li, X., 2015. Object-based urban tree species classification using bi-temporal worldview-2 and worldview-3 images. Rem. Sens. 7 (12), 16917–16937. https://doi.org/10.3390/rs71215861.

Li, J., Hu, B., Noland, T.L., 2013. Classification of tree species based on structural features derived from high density LiDAR data. Agric. For. Meteorol. 171 (172), 104–114. https://doi.org/10.1016/j.agrformet.2012.11.012.

Li, Q., 2021. A Two-Level Fusion Approach to Mapping Urban Tree Species Using Multispectral Imagery and LiDAR Data. Master thesis. Earth and Space Engineering, York University, Toronto, Canada.

Lin, H.T.L., Chih-Jen, Weng, Ruby C., 2007. A Note on Platt's Probabilistic Outputs for Support Vector Machines, vols. 267–276. https://doi.org/10.1007/s10994-007-5018-6.

Liu, Z., Dezert, J., Pan, Q., Mercier, G., 2011. Combination of sources of evidence with different discounting factors based on a new dissimilarity measure. Decis. Support Syst. 52 (1), 133–141. https://doi.org/10.1016/j.dss.2011.06.002.

Maxwell, A.E., Warner, T.A., Fang, F., 2018. Implementation of machine-learning classification in remote sensing: an applied review. Int. J. Rem. Sens. 39 (9), 2784–2817. https://doi.org/10.1080/01431161.2018.1433343.

Mora, B., Fournier, R.A., Foucher, S., 2011. Application of evidential reasoning to improve the mapping of regenerating forest stands. Int. J. Appl. Earth Obs. Geoinf. 13 (3), 458–467. https://doi.org/10.1016/j.jag.2010.10.001.

Mora, B., Fournier, R.A., Foucher, S., 2012. Mapping the health of mature deciduous forest stands by fusing multisource geospatial data with Dempster's combination rule. Int. J. Rem. Sens. 33 (4), 1139–1163. https://doi.org/10.1080/01431161.2010.550644.

Murphy, C.K., 2000. Combining belief functions when evidence conflicts. Decis. Support Syst. 29 (1), 1–9. https://doi.org/10.1016/S0167-9236(99)00084-6.

Pittman, R., Hu, B., Webster, K., 2021. Improvement of soil property mapping in the Great Clay Belt of northern Ontario using multi-source remotely sensed data. Geoderma 381, 114761. https://doi.org/10.1016/j.geoderma.2020.114761.

Platt, J., 1999. Probabilistic outputs for support vector machines and comparisons to regularized likelihood methods. Adv. Large Margin Classifiers 10 (3), 61–74.

Shafer, G., 1976. A Mathematical Theory of Evidence, vol. 42. Princeton university press.

Smets, P., 2000. Data fusion in the transferable belief model. In: Proceedings of the Third International Conference on Information Fusion, 1, pp. PS21–PS33. https://doi.org/10.1109/IFIC.2000.862713.

Stavrakoudis, D.G., Dragozi, E., Gitas, I.Z., Karydas, C.G., 2014. Decision fusion based on hyperspectral and multispectral satellite imagery for accurate forest species mapping. Rem. Sens. 6 (8), 6897–6928. https://doi.org/10.3390/rs6086897.

Wu, T.-F., Lin, C.-J., Weng, R.C., 2004. Probability estimates for multi-class classification by pairwise coupling. J. Mach. Learn. Res. 5 (Aug), 975–1005.

Yong, D., Wenkang, S., Zhenfu, Z., Qi, L., 2004. Combining belief functions based on distance of evidence. Decis. Support Syst. 38 (3), 489–493. https://doi.org/10.1016/j.dss.2004.04.015.

Zadeh, L., 1986. A simple view of the Dempster-Shafer theory of evidence and its implication for the rule of combination. AI Mag. 7 (2), 85–90.

Zhang, K., Hu, B., 2012. Individual urban tree species classification using very high spatial resolution airborne multi-spectral imagery using longitudinal profiles. Rem. Sens. 4 (6), 1741–1757. https://doi.org/10.3390/rs4061741.